THE JOURNAL OF PHYSICAL CHEMISTRY Letters

Letter

pubs.acs.org/JPCL

Multi-Timescale Dynamics in Intrinsically Disordered Proteins from NMR Relaxation and Molecular Simulation

Nicola Salvi, Anton Abyzov, and Martin Blackledge*

Institut de Biologie Structurale, CEA, CNRS, University Grenoble Alpes, Grenoble 38044, France

Supporting Information

ABSTRACT: Intrinsically disordered proteins (IDPs) access highly diverse ensembles of conformations in their functional states. Although this conformational plasticity is essential to their function, little is known about the dynamics underlying interconversion between accessible states. Nuclear magnetic resonance (NMR) relaxation rates contain a wealth of information about the time scales and amplitudes of motion in IDPs, but the highly dynamic nature of IDPs complicates their interpretation. We present a novel framework in which a series of molecular dynamics (MD) simulations are used in combination with experimental ^{15}N relaxation measurements to characterize the ensemble of dynamic processes contributing to the observed rates. By accounting for the distinct dynamic averaging present in the different conformational states sampled by the equilibrium ensemble, we are able to accurately describe both dynamic time scales and local and global conformational sampling. The method is robust, systematically improving agreement with independent experimental relaxation data, irrespective of the actively targeted rates, and suggesting interdependence of motions occurring on time scales varying over 3 orders of magnitude.

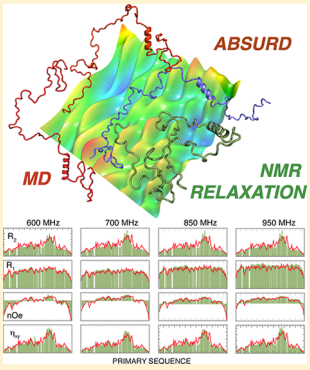

Intrinsically disordered proteins (IDPs) are highly flexible in their functional state,[1−3] sampling a much flatter energy landscape than their folded counterparts and allowing interconversion between a quasi-continuum of accessible conformations. Their extreme conformational plasticity provides them with the unique capability of acting in functional modes that are not achievable by folded proteins, such as folding-upon-binding,[4] folding into different conformations depending on binding partner, or the formation of dynamic complexes.[5]

In order to understand the relationship between dynamics and function in IDPs, it is necessary to describe their behavior at atomic resolution. The conformational space sampled by IDPs can be described in terms of ensembles of rapidly interconverting structures, and nuclear magnetic resonance (NMR) is the method of choice for the experimental characterization of representative ensembles of states.[6,7] On the basis of conformationally averaged first order interactions, such as chemical shifts and scalar and dipolar couplings, it is possible to develop a relatively precise idea of the populations of states sampled on time scales that interconvert faster than hundreds of microseconds.[8−13] Nevertheless, although it is becoming progressively clearer how to represent the conformational space sampled by IDPs,[14−16] little is known about the dynamics within, and interconversion between, these conformational states.

^{15}N spin relaxation rates are sensitive to local and long-range reorientational dynamics occurring on time scales from tens of picoseconds to tens of nanoseconds[17] and have been used extensively to study the motional properties of unfolded proteins.[18−27] However, the assignment of conformational modes associated with different time scales from spin relaxation data alone is highly challenging, requiring, for example, extensive sets of data acquired at multiple magnetic fields and temperatures.[28] The combination of NMR relaxation with molecular dynamics (MD) simulation offers the possibility of describing motional modes and time scales with otherwise inaccessible precision.[29−32]

In practice, the characteristic time scales of motions affecting NMR relaxation measurements make this combination particularly challenging in highly flexible systems such as IDPs. Each relaxation rate reports on the population-weighted average over all accessible states sampled up to the millisecond. For conformational exchange faster than the chemical shift time scale, which is generally the case for IDPs in solution, the observed relaxation rate is given by the average $\langle R \rangle = \sum_i x_i R^i$, in which x_i and R^i are the population and the relaxation rate of state i, respectively. The rate R^i within each substate is defined by the angular correlation function $C_i(\tau)$, dependent on the local properties of the energy landscape around this local minimum, which is eventually quenched by relaxation active angular fluctuations occurring up to the tens of nanoseconds. In principle it would be necessary to run MD simulations, and explicitly calculate $C_i(\tau)$ (and R^i) for all of available states that interconvert on time scales faster than the chemical shift coalescence limit (milliseconds), and average the individual rates as a function of their populations. Indeed, within the framework of folded proteins, the description of rapidly interconverting conformational substates with the same overall

Received: April 25, 2016
Accepted: June 14, 2016
Published: June 14, 2016

DOI: 10.1021/acs.jpclett.6b00885
J. Phys. Chem. Lett. 2016, 7, 2483−2489

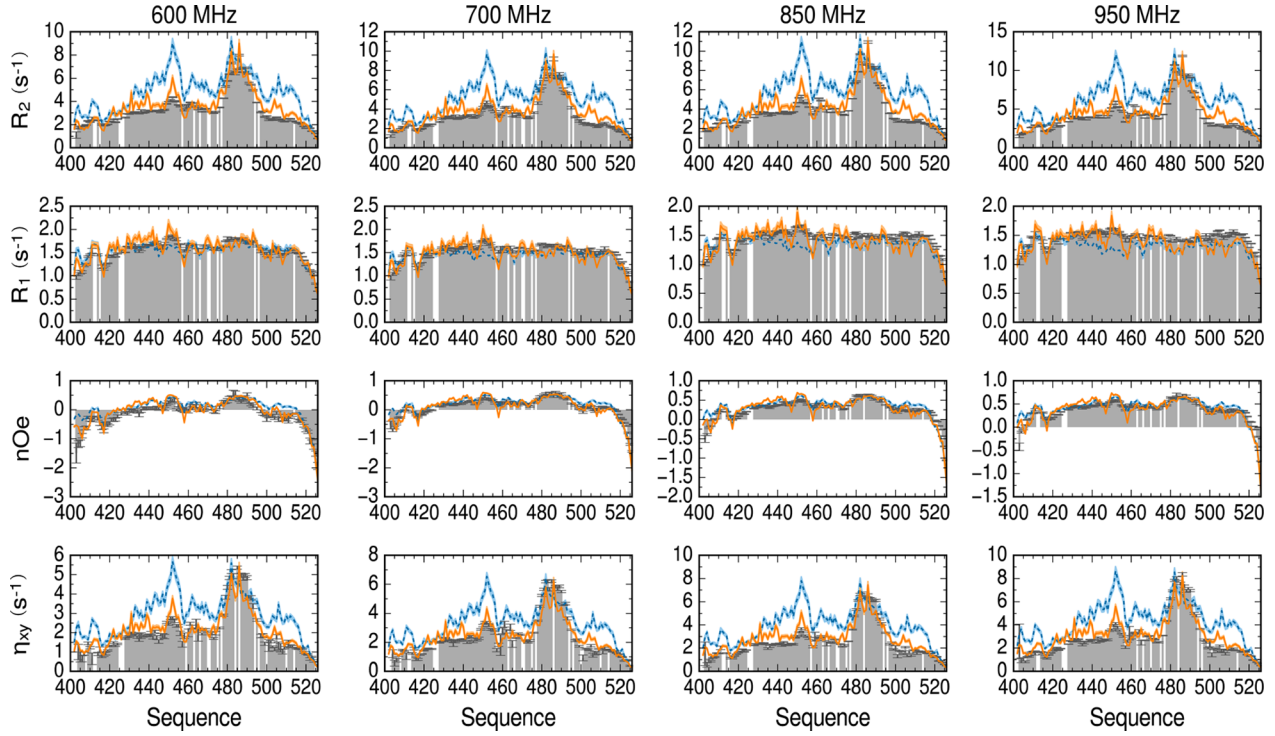

Figure 1. Experimental ^{15}N transverse relaxation rates R_2, longitudinal relaxation rates R_1, heteronuclear nOe ratios and CSA/DD transverse cross-correlated cross-relaxation rates η_{xy} measured at 600, 700, 850, and 950 MHz (gray bars) are poorly reproduced by the rates calculated from Simulation **1** (blue dashed line). All rates calculated after applying the ABSURD procedure (in this case applied to R_2 measured at 850 MHz (orange line)) are in better agreement with the experimental data.

fold but distinct internal dynamic modes has been shown to significantly improve reproduction of measured relaxation rates.[33,34] In IDPs, the constraints on the accuracy of MD-based sampling are much more challenging, both in terms of calculation time and, equally, in terms of population of substates and completeness of sampling.[35]

In this study, we present an innovative framework that combines MD simulation with NMR spin relaxation to characterize the dynamic behavior of IDPs. Analysis of several long, fully solvated trajectories (a total of 6.5 μs) of a 126 amino acid IDP demonstrates that standard MD simulations of microsecond length fail to describe motions that are most influenced by inaccuracies in the hydrodynamics of the peptide chain.[36,37] To address this problem, we explicitly mimic the heterogeneous conformational origin of experimentally measured relaxation rates, by identifying weighted combinations of $C_i(\tau)$, derived from distinct regions of a series of trajectories starting from different basins in the energy landscape, thereby extending the concept of ensemble-descriptions into an additional dimension, time. Explicit incorporation of the distinct dynamic averaging present throughout the conformational ensemble greatly improves agreement with independent relaxation data, while improving agreement with local and global conformational sampling properties.

Our test scenario is the study of the protein intrinsically disordered C-terminal domain (NT) of the nucleoprotein of Sendai virus that packages the viral RNA genome within the nucleocapsid.[38] The interaction site of NT (residues 476−492) has been shown to sample an equilibrium of different helical conformations (75% of the conformers in the ensemble) and a completely unfolded state (25%).[39,40] Upon interaction with the viral phosphoprotein, the helical recognition element binds via a distinct conformational funneling pathway.[41,42] Simulation of the relaxation active motional behavior of the protein presents a particular challenge because of the heterogeneous conformational equilibrium between partially folded helical and unfolded states.

Because of the expected importance of protein−solvent interactions for the accurate simulation of IDPs,[37,43,44] two sets of MD simulations were performed using different state-of-the-art force field descriptions of water. Simulation **1** comprises ten 250 ns trajectories initiated from randomly selected members of a representative ensemble describing the free energy basins sampled by the helical element (U = unfolded, helices H1, H2, and H3). Simulation **2** consists of four 1.0 μs MD simulations initiated from conformers of NT randomly selected from the ensemble. AMBER ff99SB-ILDN[45] was used in all simulations, in conjunction with the TIP4P/2005[43] and TIP4P-D[37] water models for simulations **1** and **2** respectively. Approximately 84 000 water molecules were used in a rhombic dodecahedral box.

Covariance matrix analysis[46] indicates that the magnitude of fluctuations of internal coordinates depends little on starting conformation, except for residues 476−492 in the helical region (Supporting Figure S1). Helical persistence fluctuates over the different trajectories on the 100 ns time scales in TIP4P-D water (Supporting Figure S2), whereas simulations using TIP4P/2005 sustain starting helical conformations over the entire trajectory.

Angular order parameters S^2_{NH} were calculated over each trajectory, identifying incomplete convergence ($S^2_{NH} > 0.01$) in all cases, even in the unfolded parts of the chain (Supporting Figure S3). This is initially surprising, as the dominant time scale of motions detected by NMR relaxation in IDPs occurs on the order of nanoseconds,[28] hundreds of times shorter than these trajectories. However, if we consider that dynamics from a

DOI: 10.1021/acs.jpclett.6b00885
J. Phys. Chem. Lett. 2016, 7, 2483−2489

quasi-continuum of disordered states contribute simultaneously to the measured relaxation, it is perhaps not surprising that a single trajectory cannot sample the conformational space accessed by the protein sufficiently broadly to achieve convergence. Interestingly S^2_{NH} calculated after 500 ns and 1.0 μs in any of the independent trajectories are also almost identical, suggesting that sampling for longer times does not measurably improve convergence. We postulate that the associated poor reproduction of different experimental spin relaxation rates from the trajectories (Figure 1 for Simulation **1** and Supporting Figure S5 for Simulation **2**) results from sampling of conformational space within single trajectories that is non-native or at least over-represented. Special hardware can access much longer trajectories than those used here, although we note that even the recent 100 ms simulation of partially folded ACBP required additional damping of the autocorrelation function (<0.02) to avoid truncation artifacts induced by residual order.[31]

We propose a different strategy, whereby conformational heterogeneity is actively appropriated to mimic the true ensemble averaging and improve the description of the averaged autocorrelation functions $\langle C(\tau)\rangle$ detected by the measured relaxation rates. To achieve this aim, $C_i(\tau)$ was calculated from subtrajectories from each simulation, probing long-enough time scales such that relaxation-active motions were sufficiently sampled ($\tau_{max} \leq 50$ or 62.5 ns for simulations **1** and **2**, respectively, following recent analysis showing that all motional modes sampled by NMR relaxation at 25 °C in NT occur on time scales <10 ns[28]). Each trajectory is thus divided into four overlapping blocks of 100 ns (simulation **1**, starting at $t_{0,k} = (k-1)\cdot 50$ ns, ($k = 1-4$), resulting in a total of 40 blocks) or eight nonoverlapping blocks of 125 ns (simulation **2**, starting at $t_{0,k} = (k-1)\cdot 125$ ns, ($k = 1-8$), resulting in a total of 32 blocks). For each block $C_i(\tau)$ is then described as a sum of $N = 128$ exponentials $e^{-\tau/\tau_{c,i}}$ whose amplitudes A_i are obtained using a Tikhonov regularization procedure.[47] For each block, the spectral densities are then defined as

$$J_i(\omega) = \sum_{i=1}^{N} \frac{A_i \tau_{c,i}}{1 + \omega^2 \tau_{c,i}^2} \quad (1)$$

and used to predict spin relaxation rates.

Optimum weights (w_i) are determined for each block by comparing the appropriately averaged relaxation rates to experimental values (see Methods section in SI). The procedure, named ABSURD (Average Block Selection Using Relaxation Data), is optimized here using a basin-hopping algorithm to minimize the residual sum of squares (RSS)

$$\mathrm{RSS} = \sum_k \sum_n \left(R_k^{\exp}(n) - \sum_i w_i \cdot R_k^i(n)\right)^2 \quad (2)$$

where indices k and n identify the kind of relaxation rate and the magnetic field used for the optimization procedure. The method relates to classical ensemble-selection approaches, with the important distinction that, in this case, each member of the ensemble represents an entire time-dependent subtrajectory containing both structural and dynamic information.

ABSURD was tested as follows. Simulated target relaxation rates were initially calculated from four randomly selected target regions of the four trajectories in simulation **2**, and averaged using arbitrary weights. ABSURD was then applied to optimize the weights of all subtrajectories by optimizing eq 2 against a single simulated rate (η_{xy} at 850 MHz). Remarkably the four target subtrajectories are correctly identified and their populations quantitatively reproduced, with all other populations effectively zero, even in the case of adjacent subtrajectories (Supporting Information Figure S4). This test calculation demonstrates that there is sufficient information contained in a single relaxation rate to discriminate between the conformational dynamics occurring in the different parts of the four trajectories that contributed to this averaged relaxation rate.

The ABSURD procedure was then applied to the experimental data from NT, independently optimizing eq 2 against each of the 16 rates in Figure 1. Comparison with the 15 other relaxation rates measured at different magnetic field strengths or reporting on relaxation phenomena sensitive to different time scale motions, are then used uniquely as measures of cross-validation. The results of the optimization are summarized in Figures 2 and S6 for simulations **1** and **2**,

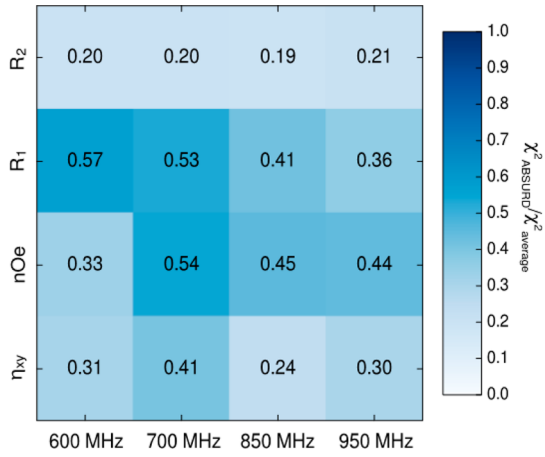

Figure 2. Ratios of χ^2 values calculated for simulation **1** before ($\chi^2_{average}$ = 262.1) and after applying ABSURD (χ^2_{ABSURD}). Selection using rates that depend predominantly on $J(0)$, such as R_2 and η_{xy}, effectively improves the agreement with the experimental data. Rates reporting on motions at shorter time scales (R_1 and nOe) are less effective.

respectively. In general, selection using η_{xy} and R_2 provides better overall reproduction of rates than heteronuclear nOe or R_1, suggesting that ABSURD selects for segments of the trajectories in which the spurious contacts that increase the compactness of the structure and, consequently, $J(0)$, are removed. Very similar weights are determined using η_{xy} and R_2 rates (Figures S7 and S8), whereas selection against heteronuclear NOE and R_1, which reports on faster time scale motions, favors an overlapping set of blocks. For each relaxation rate, the optimal weights do not depend significantly on the magnetic field.

Similar features are seen for both simulation **1** (Figure 1) and simulation **2** (Supporting Figure S5), with significant improvement in the prediction of relaxation rates sensitive to motions on all sampled time scales in comparison to the calculation of average rates over the complete 250 ns (or 1.0 μs) trajectories. In particular, in the optimally weighted ensemble of trajectories the region between 420 and 470 no longer exhibits spurious contributions to rates dominated by slow motions (R_2 and η_{xy}) that are not seen in the experimental data.

Although it is not surprising that selection against R_2 improves predicted η_{xy}, as both depend predominantly on $J(0)$, prediction of nOe and R_1 values, reporting on motions on

DOI: 10.1021/acs.jpclett.6b00885
J. Phys. Chem. Lett. 2016, 7, 2483−2489

100s of picoseconds and nanosecond time scales, also show systematic and significant improvement (Figures S9–S10) (with the exception of R_1 in simulation **2**). This observation indicates that identification of the appropriate parts of the trajectories necessary to reproduce $J(0)$ is essential for reproduction of motions on all relaxation-active time scales, providing evidence for a correlation between motions occurring on these significantly different time scales. Further inspection indicates that the selection effectively removes errors introduced by oversampled transient hydrophobic interaction in the region around W449 (Figure S11).

In order to verify the effect of the ABSURD selection on the conformational sampling we compared the selected ensemble of structures present in each subtrajectory after selection with independent experimental observables that are sensitive to local and long-range conformational sampling. Global dimensions are in good agreement, as estimated by comparison to experimental SAXS curves (Figure S12). Similarly, experimental chemical shifts are well reproduced throughout the protein by simulation **1** both without and with ABSURD selection (Figure 3), despite the disagreement of the non-selected ensemble with

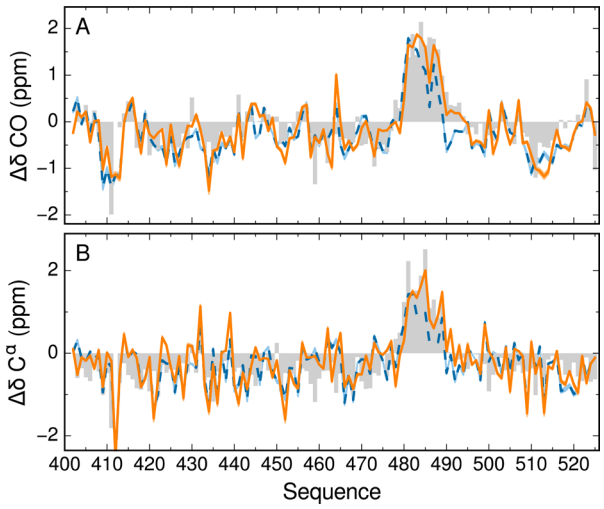

Figure 3. $^{13}C'$ (A) and $^{13}C\alpha$ (B) secondary chemical shifts. Experimental data (gray bars) are compared with values predicted from simulation **1** before (dashed blue line) and after ABSURD-selection using R_2 (850 MHz) as the target in eq 2 (orange line).

measured relaxation (Figure 1), serving as a reminder that agreement with local backbone sampling does not guarantee accuracy of dynamics. A significant improvement in chemical shift prediction from throughout the helical region (residues 476–492) is nevertheless observed after ABSURD selection. Overall therefore, ABSURD selection only marginally modifies the local conformational space that is sampled, but drastically affects the transition time scales between different conformational states. We note that the TIP4P-D force field used in simulation **2** (Figure S13) poorly reproduces the helical propensity, as a consequence of the instability of the secondary structural elements using this water model (Figure S2).

The selected ensemble of subtrajectories were compared with the results of a recent study,[28] where a model-free (MF) analysis of data acquired at multiple fields and temperatures (a subset of which are used in the present work) revealed that the complex conformational rearrangements in NT can be mapped onto three time scales, reporting on slow solvent-dependent motions, intermediate backbone dihedral angle dynamics, and fast librational modes. Figures S14 and S15 show that motions on similar time scales as those derived from the MF analysis are present in both simulations **1** and **2** after selection using ABSURD. In order to make a more quantitative comparison, ABSURD-optimized correlation times were grouped into three clusters (fast, intermediate, and slow), depending on the closest MF-derived time scale (Figures S14 and S15). For each cluster an effective amplitude, given by the sum of the amplitudes of all the members of the cluster, and an effective time scale, given by the average of the correlation times belonging to the cluster weighted by their amplitudes, were calculated. These quantities are compared directly with the MF results in Figures 4 and S16 for simulations **1** and **2**, respectively.

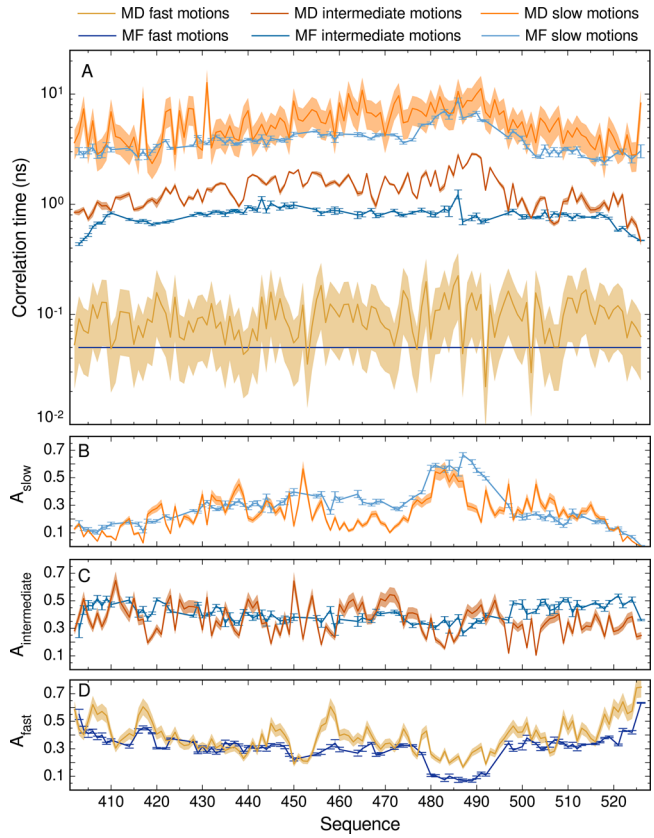

Figure 4. Clustered correlation times (A) and their amplitudes (B–D) in the blocks of simulation **1** selected by ABSURD using R_2 (850 MHz) are compared with the corresponding quantities derived directly from the experimental data.[28]

Motional time scales of all three components agree broadly with those derived from MF analysis (Figure 4A), albeit with slightly slower predicted intermediate motions. The ABSURD-selected ensemble of trajectories convincingly reproduces the differences in slow motions between the unfolded and helical regions of the protein. The relative amplitudes of the three components are also well reproduced (Figure 4B–D). Similar time scales are obtained for simulation **2** (Figure S16), however, the motional amplitudes less convincingly show the specific dynamics of residues 476–492, supporting the suggestion that both conformational and dynamic properties of structured segments of NT are not accurately simulated in TIP4P-D.

DOI: 10.1021/acs.jpclett.6b00885
J. Phys. Chem. Lett. 2016, 7, 2483–2489

In conclusion, we present a framework for the interpretation of experimental NMR relaxation data in solution, providing a detailed and accurate description of the dynamic time scales, amplitudes and nature of motions in IDPs. This approach determines weights of dynamic subtrajectories from a broadly sampled combination of MD simulations, nucleated from very diverse conformations, to develop an ensemble description of the conformationally averaged time-dependent autocorrelation functions. The method thereby mimics the ensemble-averaging intrinsic to experimentally measured relaxation rates, combining distinct time-dependent correlation functions from an ensemble of substates. ABSURD is conceptually fully distinct from existing sample-and-select approaches, where combinations of single conformers are used to match chemical shifts or dipolar and scalar couplings. There is no time scale information available from such parameters that are averaged over all conformations contributing to the chemical shift average. By contrast, NMR relaxation is strongly dependent on the time scale of angular fluctuations, with distinct averaging characteristics depending on whether motions occur on time scales that are shorter or longer than the quenching of the autocorrelation function. The approach described here specifically accounts for these distinct averaging phenomena in a way that is not available to existing ensemble selection procedures.[7,8,10,13,48−50]

Reassuringly, the approach satisfactorily reproduces a large set of NMR relaxation rates that are sensitive to motions varying over nearly 3 orders of magnitude (50−100 ps to 10 ns) even when the only selection criterion is agreement with rates that are mainly dependent on local conformation and slower (5−10 ns) time scale motions. Combining only one set of relaxation rates (equivalent to one experiment) with MD significantly improves the reproduction of motional descriptions over a vast range of time scales and provides insight comparable to that obtained by more conventional model-free approaches using over 60 spin relaxation rates per residue.

ABSURD has been developed to overcome current limitations of MD simulations of disordered systems. However, it can also be used in studies of folded proteins, particularly when the interpretation of experimental data is hindered by the presence of motions that are too slow to be accessed by MD. Finally, the ability to identify ensembles of trajectories in agreement with the dynamic processes intrinsic to the protein and to filter trajectories that show nonphysical behavior, suggests that in addition to providing insight into the molecular origin of NMR relaxation in IDPs, this approach can be exploited to further improve available force fields for IDPs and more generally in the interpretation of additional time-dependent parameters such as single molecule fluorescence.[51,52]

■ ASSOCIATED CONTENT

Supporting Information

The Supporting Information is available free of charge on the ACS Publications website at DOI: 10.1021/acs.jpclett.6b00885.

Simulation details and additional details of the ABSURD analysis. Additional figures showing secondary and long-range structural features of simulations, ABSURD selection using different relaxation rates, correlation plots showing reproduction of rates not used in the selection, figures showing chemical shifts and SAXS calculations from the trajectories and selections. (PDF)

■ AUTHOR INFORMATION

Corresponding Author

*E-mail: martin.blackledge@ibs.fr.

Author Contributions

(N.S. and A.A.) These authors contributed equally to the work.

Notes

The authors declare no competing financial interest.

■ ACKNOWLEDGMENTS

The authors thank M. R. Jensen and L. Salmon for fruitful discussions. N.S. acknowledges a Swiss National Science Foundation Early Postdoc.Mobility Fellowship (P2ELP2_148858). This research was supported by the CEA (Commissariat à l'Energie Atomique et aux Energies Alternatives) and CNRS (Centre National de la Recherche Scientifique), ANR Grant ComplexDynamics (M.B.). MD simulations were performed using the HPC resources of CCRT available by GENCI (Grand Equipement National de Calcul Intensif, projects t2015077486 and t2016077486). This work used platforms of the Grenoble Instruct centre (ISBG; UMS 3518 CNRS-CEA-UJF-EMBL) with support from FRISBI (ANR-10-INSB-05-02) and GRAL (ANR-10-LABX-49-01) within the Grenoble Partnership for Structural Biology (PSB).

■ REFERENCES

(1) Uversky, V. N. Natively Unfolded Proteins: A Point Where Biology Waits for Physics. *Protein Sci.* **2002**, *11* (4), 739−756.

(2) Dunker, A. K.; Brown, C. J.; Lawson, J. D.; Iakoucheva, L. M.; Obradović, Z. Intrinsic Disorder and Protein Function. *Biochemistry* **2002**, *41* (21), 6573−6582.

(3) Dyson, H. J.; Wright, P. E. Coupling of Folding and Binding for Unstructured Proteins. *Curr. Opin. Struct. Biol.* **2002**, *12* (1), 54−60.

(4) Dyson, H. J.; Wright, P. E. Intrinsically Unstructured Proteins and Their Functions. *Nat. Rev. Mol. Cell Biol.* **2005**, *6* (3), 197−208.

(5) Tompa, P.; Fuxreiter, M. Fuzzy Complexes: Polymorphism and Structural Disorder in Protein-Protein Interactions. *Trends Biochem. Sci.* **2008**, *33* (1), 2−8.

(6) Dyson, H. J.; Wright, P. E. Unfolded Proteins and Protein Folding Studied by NMR. *Chem. Rev.* **2004**, *104* (8), 3607−3622.

(7) Jensen, M. R.; Zweckstetter, M.; Huang, J.; Blackledge, M. Exploring Free-Energy Landscapes of Intrinsically Disordered Proteins at Atomic Resolution Using NMR Spectroscopy. *Chem. Rev.* **2014**, *114* (13), 6632−6660.

(8) Mittag, T.; Forman-Kay, J. D. Atomic-Level Characterization of Disordered Protein Ensembles. *Curr. Opin. Struct. Biol.* **2007**, *17* (1), 3−14.

(9) Nodet, G.; Salmon, L.; Ozenne, V.; Meier, S.; Jensen, M. R.; Blackledge, M. Quantitative Description of Backbone Conformational Sampling of Unfolded Proteins at Amino Acid Resolution from NMR Residual Dipolar Couplings. *J. Am. Chem. Soc.* **2009**, *131* (49), 17908−17918.

(10) Allison, J. R.; Varnai, P.; Dobson, C. M.; Vendruscolo, M. Determination of the Free Energy Landscape of Alpha-Synuclein Using Spin Label Nuclear Magnetic Resonance Measurements. *J. Am. Chem. Soc.* **2009**, *131* (51), 18314−18326.

(11) Salmon, L.; Nodet, G.; Ozenne, V.; Yin, G.; Jensen, M. R.; Zweckstetter, M.; Blackledge, M. NMR Characterization of Long-Range Order in Intrinsically Disordered Proteins. *J. Am. Chem. Soc.* **2010**, *132* (24), 8407−8418.

(12) Schwalbe, M.; Ozenne, V.; Bibow, S.; Jaremko, M.; Jaremko, L.; Gajda, M.; Jensen, M. R.; Biernat, J.; Becker, S.; Mandelkow, E.; et al. Predictive Atomic Resolution Descriptions of Intrinsically Disordered hTau40 and α-Synuclein in Solution from NMR and Small Angle Scattering. *Structure* **2014**, *22* (2), 238−249.

(13) Mantsyzov, A. B.; Maltsev, A. S.; Ying, J.; Shen, Y.; Hummer, G.; Bax, A. A Maximum Entropy Approach to the Study of Residue-

DOI: 10.1021/acs.jpclett.6b00885
J. Phys. Chem. Lett. 2016, 7, 2483−2489

Specific Backbone Angle Distributions in α-Synuclein, an Intrinsically Disordered Protein. *Protein Sci.* **2014**, *23* (9), 1275−1290.
(14) Eliezer, D. Biophysical Characterization of Intrinsically Disordered Proteins. *Curr. Opin. Struct. Biol.* **2009**, *19* (1), 23−30.
(15) Fisher, C. K.; Stultz, C. M. Constructing Ensembles for Intrinsically Disordered Proteins. *Curr. Opin. Struct. Biol.* **2011**, *21* (3), 426−431.
(16) Jensen, M. R.; Ruigrok, R. W. H.; Blackledge, M. Describing Intrinsically Disordered Proteins at Atomic Resolution by NMR. *Curr. Opin. Struct. Biol.* **2013**, *23* (3), 426−435.
(17) Palmer, A. NMR Characterization of the Dynamics of Biomacromolecules. *Chem. Rev.* **2004**, *104* (8), 3623−3640.
(18) Alexandrescu, A.; Shortlet, D. Backbone Dynamics of a Highly Disordered 131-Residue Fragment of Staphylococcal Nuclease. *J. Mol. Biol.* **1994**, *242* (4), 527−546.
(19) Yang, D. W.; Mok, Y. K.; FormanKay, J. D.; Farrow, N. A.; Kay, L. E. Contributions to Protein Entropy and Heat Capacity from Bond Vector Motions Measured by NMR Spin Relaxation. *J. Mol. Biol.* **1997**, *272* (5), 790−804.
(20) Buevich, A. V.; Baum, J. Dynamics of Unfolded Proteins: Incorporation of Distributions of Correlation Times in the Model Free Analysis of NMR Relaxation Data. *J. Am. Chem. Soc.* **1999**, *121* (37), 8671−8672.
(21) Yao, J.; Chung, J.; Eliezer, D.; Wright, P. E.; Dyson, H. J. NMR Structural and Dynamic Characterization of the Acid-Unfolded State of Apomyoglobin Provides Insights into the Early Events in Protein Folding. *Biochemistry* **2001**, *40* (12), 3561−3571.
(22) Ochsenbein, F.; Neumann, J. M.; Guittet, E.; Van Heijenoort, C. Dynamical Characterization of Residual and Non-Native Structures in a Partially Folded Protein by N-15 NMR Relaxation Using a Model Based on a Distribution of Correlation Times. *Protein Sci.* **2002**, *11* (4), 957−964.
(23) Klein-Seetharaman, J.; Oikawa, M.; Grimshaw, S. B.; Wirmer, J.; Duchardt, E.; Ueda, T.; Imoto, T.; Smith, L. J.; Dobson, C. M.; Schwalbe, H. Long-Range Interactions within a Nonnative Protein. *Science* **2002**, *295* (5560), 1719−1722.
(24) Choy, W.-Y.; Kay, L. E. Probing Residual Interactions in Unfolded Protein States Using NMR Spin Relaxation Techniques: An Application to Δ131Δ. *J. Am. Chem. Soc.* **2003**, *125* (39), 11988−11992.
(25) Modig, K.; Poulsen, F. M. Model-Independent Interpretation of NMR Relaxation Data for Unfolded Proteins: The Acid-Denatured State of ACBP. *J. Biomol. NMR* **2008**, *42* (3), 163−177.
(26) Gill, M. L.; Byrd, R. A.; Arthur, G.; Palmer, I. I. I. Dynamics of GCN4 Facilitate DNA Interaction: A Model-Free Analysis of an Intrinsically Disordered Region. *Phys. Chem. Chem. Phys.* **2016**, *18*, 5839−5849.
(27) Khan, S. N.; Charlier, C.; Augustyniak, R.; Salvi, N.; Dejean, V.; Bodenhausen, G.; Lequin, O.; Pelupessy, P.; Ferrage, F. Distribution of Pico- and Nanosecond Motions in Disordered Proteins from Nuclear Spin Relaxation. *Biophys. J.* **2015**, *109* (5), 988−999.
(28) Abyzov, A.; Salvi, N.; Schneider, R.; Maurin, D.; Ruigrok, R. W. H.; Jensen, M. R.; Blackledge, M. Identification of Dynamic Modes in an Intrinsically Disordered Protein Using Temperature-Dependent NMR Relaxation. *J. Am. Chem. Soc.* **2016**, *138* (19), 6240−6251.
(29) Prompers, J. J.; Bruschweiler, R. General Framework for Studying the Dynamics of Folded and Nonfolded Proteins by NMR Relaxation Spectroscopy and MD Simulation. *J. Am. Chem. Soc.* **2002**, *124* (16), 4522−4534.
(30) Xue, Y.; Skrynnikov, N. R. Motion of a Disordered Polypeptide Chain as Studied by Paramagnetic Relaxation Enhancements, 15N Relaxation, and Molecular Dynamics Simulations: How Fast Is Segmental Diffusion in Denatured Ubiquitin? *J. Am. Chem. Soc.* **2011**, *133* (37), 14614−14628.
(31) Lindorff-Larsen, K.; Trbovic, N.; Maragakis, P.; Piana, S.; Shaw, D. E. Structure and Dynamics of an Unfolded Protein Examined by Molecular Dynamics Simulation. *J. Am. Chem. Soc.* **2012**, *134* (8), 3787−3791.
(32) Robustelli, P.; Trbovic, N.; Friesner, R. A.; Palmer, A. G. Conformational Dynamics of the Partially Disordered Yeast Transcription Factor GCN4. *J. Chem. Theory Comput.* **2013**, *9* (11), 5190−5200.
(33) Markwick, P. R. L.; Bouvignies, G.; Salmon, L.; McCammon, J. A.; Nilges, M.; Blackledge, M. Toward a Unified Representation of Protein Structural Dynamics in Solution. *J. Am. Chem. Soc.* **2009**, *131* (46), 16968−16975.
(34) Guerry, P.; Salmon, L.; Mollica, L.; Ortega Roldan, J.-L.; Markwick, P.; van Nuland, N. A. J.; McCammon, J. A.; Blackledge, M. Mapping the Population of Protein Conformational Energy Sub-States from NMR Dipolar Couplings. *Angew. Chem., Int. Ed.* **2013**, *52* (11), 3181−3185.
(35) Rauscher, S.; Gapsys, V.; Gajda, M. J.; Zweckstetter, M.; de Groot, B. L.; Grubmüller, H. Structural Ensembles of Intrinsically Disordered Proteins Depend Strongly on Force Field: A Comparison to Experiment. *J. Chem. Theory Comput.* **2015**, *11* (11), 5513−5524.
(36) Best, R. B.; Zheng, W.; Mittal, J. Balanced Protein-Water Interactions Improve Properties of Disordered Proteins and Non-Specific Protein Association. *J. Chem. Theory Comput.* **2014**, *10* (11), 5113−5124.
(37) Piana, S.; Donchev, A. G.; Robustelli, P.; Shaw, D. E. Water Dispersion Interactions Strongly Influence Simulated Structural Properties of Disordered Protein States. *J. Phys. Chem. B* **2015**, *119* (16), 5113−5123.
(38) Communie, G.; Ruigrok, R. W.; Jensen, M. R.; Blackledge, M. Intrinsically Disordered Proteins Implicated in Paramyxoviral Replication Machinery. *Curr. Opin. Virol.* **2014**, *5*, 72−81.
(39) Jensen, M. R.; Blackledge, M. On the Origin of NMR Dipolar Waves in Transient Helical Elements of Partially Folded Proteins. *J. Am. Chem. Soc.* **2008**, *130* (34), 11266−11267.
(40) Jensen, M. R.; Houben, K.; Lescop, E.; Blanchard, L.; Ruigrok, R. W. H.; Blackledge, M. Quantitative Conformational Analysis of Partially Folded Proteins from Residual Dipolar Couplings: Application to the Molecular Recognition Element of Sendai Virus Nucleoprotein. *J. Am. Chem. Soc.* **2008**, *130* (25), 8055−8061.
(41) Houben, K.; Marion, D.; Tarbouriech, N.; Ruigrok, R. W. H.; Blanchard, L. Interaction of the C-Terminal Domains of Sendai Virus N and P Proteins: Comparison of Polymerase-Nucleocapsid Interactions within the Paramyxovirus Family. *J. Virol.* **2007**, *81* (13), 6807−6816.
(42) Schneider, R.; Maurin, D.; Communie, G.; Kragelj, J.; Hansen, D. F.; Ruigrok, R. W. H.; Jensen, M. R.; Blackledge, M. Visualizing the Molecular Recognition Trajectory of an Intrinsically Disordered Protein Using Multinuclear Relaxation Dispersion NMR. *J. Am. Chem. Soc.* **2015**, *137* (3), 1220−1229.
(43) Abascal, J. L. F.; Vega, C. A General Purpose Model for the Condensed Phases of Water: TIP4P/2005. *J. Chem. Phys.* **2005**, *123* (23), 234505.
(44) Henriques, J.; Cragnell, C.; Skepö, M. Molecular Dynamics Simulations of Intrinsically Disordered Proteins: Force Field Evaluation and Comparison with Experiment. *J. Chem. Theory Comput.* **2015**, *11* (7), 3420−3431.
(45) Lindorff-Larsen, K.; Piana, S.; Palmo, K.; Maragakis, P.; Klepeis, J. L.; Dror, R. O.; Shaw, D. E. Improved Side-Chain Torsion Potentials for the Amber ff99SB Protein Force Field. *Proteins: Struct., Funct., Genet.* **2010**, *78* (8), 1950−1958.
(46) Hess, B. Convergence of Sampling in Protein Simulations. *Phys. Rev. E: Stat. Phys., Plasmas, Fluids, Relat. Interdiscip. Top.* **2002**, *65* (3), 31910.
(47) Urbańczyk, M.; Bernin, D.; Koźmiński, W.; Kazimierczuk, K. Iterative Thresholding Algorithm for Multiexponential Decay Applied to PGSE NMR Data. *Anal. Chem.* **2013**, *85* (3), 1828−1833.
(48) Fisher, C. K.; Stultz, C. M. Constructing Ensembles for Intrinsically Disordered Proteins. *Curr. Opin. Struct. Biol.* **2011**, *21* (3), 426−431.
(49) Affentranger, R.; Tavernelli, I.; Di Iorio, E. E. A Novel Hamiltonian Replica Exchange MD Protocol to Enhance Protein

DOI: 10.1021/acs.jpclett.6b00885
J. Phys. Chem. Lett. 2016, 7, 2483−2489

Conformational Space Sampling. *J. Chem. Theory Comput.* **2006**, *2* (2), 217−228.
(50) Sugita, Y.; Okamoto, Y. Replica-Exchange Molecular Dynamics Method for Protein Folding. *Chem. Phys. Lett.* **1999**, *314* (1−2), 141−151.
(51) Soranno, A.; Buchli, B.; Nettels, D.; Cheng, R. R.; Müller-Späth, S.; Pfeil, S. H.; Hoffmann, A.; Lipman, E. A.; Makarov, D. E.; Schuler, B. Quantifying Internal Friction in Unfolded and Intrinsically Disordered Proteins with Single-Molecule Spectroscopy. *Proc. Natl. Acad. Sci. U. S. A.* **2012**, *109* (44), 17800−17806.
(52) Milles, S.; Lemke, E. A. Mapping Multivalency and Differential Affinities within Large Intrinsically Disordered Protein Complexes with Segmental Motion Analysis. *Angew. Chem., Int. Ed.* **2014**, *53* (28), 7364−7367.

DOI: 10.1021/acs.jpclett.6b00885
J. Phys. Chem. Lett. 2016, 7, 2483−2489